LAWRENCE
LIVERMORE
NATIONAL
LABORATORY

UCRL-JRNL-208675

Impact of anomalous dispersion on the interferometer measurements of plasmas

Joseph Nilsen, Walter R. Johnson, Carlos A. Iglesias, James H. Scofield

December 17, 2004

Journal of Quantitative Spectroscopy and Radiative Transfer

Impact of anomalous dispersion on the interferometer measurements of plasmas

Joseph Nilsen[1], Walter R. Johnson[2], Carlos A. Iglesias[1], and James H. Scofield[1]

[1]Lawrence Livermore National Laboratory, Livermore, CA 94551

[2]University of Notre Dame, Notre Dame, IN 46556

Abstract

For many decades optical interferometers have been used to measure the electron density of plasmas. During the last ten years X-ray lasers in the wavelength range 14 to 47 nm have enabled researchers to use interferometers to probe even higher density plasmas. The data analysis assumes that the index of refraction is due only to the free electrons, which makes the index of refraction less than one and the electron density proportional to the number of fringe shifts. Recent experiments in Al plasmas observed plasmas with an index of refraction greater than one and made us question the validity of the usual formula for calculating the index of refraction. Recent calculations showed how the anomalous dispersion from the bound electrons can dominate the index of refraction in many types of plasma and make the index greater than one or enhance the index such that one would greatly overestimate the electron density of the plasma using interferometers. In this work we calculate the index of refraction of C, Al, Ti, and Pd plasmas for photon energies from 0 to 100 eV (12.4 nm) using a new average-atom code. The results show large variations from the free electron approximation under many different plasma conditions. We validate the average-atom code against the more detailed OPAL code for carbon and aluminum plasmas. During the next decade X-ray free electron lasers and other sources will be available to probe a wider variety of plasmas at higher densities and shorter wavelengths so understanding the index of refraction in plasmas will be even more essential.

Keywords: Interferometers; Index of refraction; Plasmas; X-ray lasers; Anomalous dispersion

Introduction

For many decades optical interferometers have been used to measure the electron density of plasmas [1]. The data analysis always assumes that the index of refraction of the plasma is due only to the free electrons [1-2]. For the interferometer experiments this implies that the electron density of the plasma is directly proportional to the number of fringe shifts in the interferometer. The index of refraction in the plasma due to the free electrons is always less than one. When X-ray lasers became available, the same assumptions were used to calculate the index of refraction as the interferometer probed even higher density plasmas using the shorter wavelengths of the X-ray lasers. The original X-ray laser interferometer [3] was demonstrated a decade ago using the 15.5 nm Ne-like Y laser at the NOVA facility at Lawrence Livermore National Laboratory (LLNL). Since then many X-ray laser interferometers [4-6], as well as a high order harmonic interferometer [7], have been built in the wavelength range of 14 to 72 nm. This covers photon energies from 17 to 89 eV. In the future we expect interferometers to be built using the VUV or X-ray free electron lasers, which will extend lasers to even shorter wavelengths [8].

Recent interferometer experiments [4,5] of Al plasmas observed the fringe lines bend in the opposite direction than was expected, indicating the index of refraction was greater than one. These experiments were done at the Advanced Photon Research Center at JAERI using the 13.9 nm Ni-like Ag laser [4] and at the COMET laser facility at LLNL using the 14.7 nm Ni-like Pd laser [5]. Analysis of the experiments showed that the anomalous dispersion from the resonance lines and absorption edges of the bound electrons have a large contribution to the index of refraction with the opposite sign as the free electrons and this explains how the index of refraction is greater than one in some Al plasmas [9]. A surprising result of the calculations is that the influence of the bound electrons on the index of refraction extends far from the absorption edges and resonance lines [9]. Resonance lines affect the index of refraction at photon

energies located orders of magnitude further from the line centers than the corresponding line widths owing to the fact that they contribute through a dispersion integral.

The original analysis [9] of the index of refraction for Al plasmas was done only for a single wavelength, 14.7 nm, which is the wavelength of the Ni-like Pd X-ray laser used in experiments at LLNL [5]. That analysis combined individual calculations done for each iso-electronic sequence of Al and assumed that all the population was in the ground state of each ionization stage. It became clear that we needed the ability to calculate the index of refraction for any plasma at any wavelength.

Fortunately we had available a version of the INFERNO average atom code that is routinely used to calculate the distribution of levels and the absorption coefficient for plasma at a given temperature and density [10]. Using a modified version of this code [11], we are now able to calculate the index of refraction for a wide range of plasma conditions. In this work we present results for C, Al, Ti, and Pd plasmas from singly to many times ionized. The index of refraction is calculated for photon energies from 0 to 100 eV (12.4 nm). These calculations enable us to understand under what plasma conditions the free electron approximation is valid and gives us an estimate of the magnitude of the bound electron contribution. We validate the average atom code results for C and Al plasmas against calculations done with the more detailed OPAL code [12-14].

Traditional analysis of interferometer experiments

The usual formula for the index of refraction of a plasma due to free electrons is $n = (1 - N_{elec} / N_{crit})^{1/2}$ where N_{elec} is the electron density of the plasma and N_{crit} is the plasma critical density. At wavelength λ, $N_{crit} = \pi / (r_0 \lambda^2)$ where r_0 is the classical electron radius, 2.818×10^{-13} cm [2]. Since experiments typically measure an electron density that is much less than the critical density the formula above is approximated by $n = 1 - (N_{elec} / 2N_{crit})$. In typical interferometer experiments [3-7] that probe plasma of length L using a source with wavelength λ, the number of fringe shifts is equal to $\int_0^L (1-n)\,ds/\lambda$. For a plasma that is uniform over length L this reduces to

$(1 - n)\ L / \lambda$. This formula assumes that the interferometer is in a vacuum where the index of refraction is 1 except for the plasma being probed and that one compares the fringe shifts against a set of reference fringes in the absence of any plasma. This also assumes that there is a small angle between the two arms of the interferometer so that the cosine of the angle between the two arms can be approximated as 1. With the above approximation for n, the number of fringe shifts equals $(N_{elec}\ L) / (2\ \lambda\ N_{crit})$. The experimental analysis is done by simply counting how far the fringes have shifted compared with the reference fringes and converting this into electron density. For the 14.7 nm Pd X-ray laser the number of fringe shifts in the interferometer is $(N_{elec}\ L) / (1.5 \times 10^{19}\ cm^{-2})$ and the critical density is $5.17 \times 10^{24}\ cm^{-3}$.

Including the bound electrons in the calculation of the index of refraction

From the anomalous results in the interferometer experiments [4,5] of the Al plasmas it is clear that the traditional technique used to analyze the interferometer experiments is incomplete. We realized that the bound electrons were playing a significant role in the index of refraction for the Al plasma.

To understand the role of the bound electrons our original analysis [9] calculated the continuum absorption cross-sections σ for each ionization stage of Al using a Hartree-Slater code. The energies were adjusted to make certain the L3 edges for the 2p electrons agreed with the experimentally measured edges for neutral, singly, doubly, and triply ionized Al. The contributions from the absorption lines were then added to the continuum absorption. For Al (+1) and Al (+2) the measured line positions and oscillator strengths from Refs. 15 and 16 for the absorption lines below the L3 edges were used. For Al (+3) the n=2 to n=3 and 2p to 4s line positions and line strengths were used from Ref. 17. The total absorption coefficient $\alpha = N_{ion}\ \sigma = (4\ \pi\ \beta) / \lambda$ where N_{ion} is the ion density of the plasma and β is the imaginary part of the complex index of refraction n* defined by

$$n^* = 1 - \delta - i\beta \qquad (1)$$

The real part of the index of refraction n = 1 – δ. Typically one tabulates the dimensional-less optical constants f_2 and f_1 which are related to δ and β by $\delta = f_1 N_{ion} / (2 N_{crit})$ and $\beta = f_2 N_{ion} / (2 N_{crit})$ [18]. From the total absorption cross-section σ we determine the optical constant $f_2 = \sigma / (2 \lambda r_0)$. We then derive the optical constant f_1 as a function of photon energy E using the Kramers-Kronig dispersion relation [19]. This involves taking the principal value of the integral.

$$f_1(E) = Z_{nuc} + \frac{2}{\pi} P.V. \int_0^\infty \frac{f_2(\varepsilon)\, \varepsilon\, d\varepsilon}{E^2 - \varepsilon^2} \qquad (2)$$

Z_{nuc} is the atomic number of the element. This means we include the total number of bound and free electrons when calculating the dispersion relation. For example, $Z_{nuc} = 13$ for an Al plasma. For neutral materials the oscillator sum rules insure that f_1 goes to zero at zero energy and Z_{nuc} at infinite energy. For an ionized plasma with average ionization Z* then $f_1 = Z^*$ at E = 0.

The real part of the index of refraction $n = 1 – [(f_1 N_{ion}) / (2 N_{crit})]$ which makes $1 – n = (f_1 N_{ion}) / (2 N_{crit})$. In the absence of any bound electrons f_1 is equivalent to the number of free electrons per ion. Table 1 shows our best calculation of the partial components and total f_1 value for each ionization stage of Al for a 14.7 nm or 84.46 eV X-ray. Taking the ratio of f1 to the number of free electrons in Table 1 gives the ratio of the measured electron density to the actual electron density. When the ratio is negative, the index of refraction is greater than one and the fringes bend the opposite direction than expected in the interferometer. The results of this calculation for Al are described in Ref. 9. This analysis was tedious, only included the ground state of each ionization stage, and did not include a distribution of ionization stages as one has in real plasma. For this reason we realized that the ability to calculate the index of refraction over a range of wavelength for any plasma condition would be a valuable tool for analyzing experiments.

Average-atom and OPAL codes used to calculate the index of refraction

For many years the average-atom technique incorporated in the INFERNO code [10] has been used to calculate the ionization conditions and absorption spectrum of plasmas under a wide variety of conditions. For finite temperatures and densities, the INFERNO code calculates a statistical population for occupation of one-electron Dirac orbitals in the plasma. In this work, we use a non-relativistic version of INFERNO to calculate bound and continuum orbitals and the corresponding self-consistent potential. Applying linear response theory to the average-atom leads to an average-atom version of the Kubo-Greenwood equation [20,21] for the frequency-dependent conductivity of the plasma. Molecular orbital versions of the Kubo-Greenwood formula have also been used in recent years to study the conductivity of Al plasmas [22,23]. The imaginary part of the complex dielectric function is proportional to the conductivity. The real part of the dielectric function can be found from its imaginary part using a Kramers-Kronig [19] dispersion relation. With the resulting frequency-dependent dielectric function in hand, optical properties of the plasma, such as its index of refraction and absorption coefficients, are completely determined from the dielectric function. The details of the Kubo-Greenwood formula applied to the average-atom model are described in a separate work [11].

To help validate the average-atom results we compare them against calculations done with the OPAL code [12-14]. The OPAL code was developed at the Lawrence Livermore National Laboratory to compute opacities of low- to mid-Z elements. The calculations are based on a physical picture approach that carries out a many-body expansion of the grand canonical partition function. The method includes electron degeneracy and the leading quantum diffraction term as well as systematic corrections necessary for strongly-coupled plasma regimes. The atomic data are obtained from a parametric potential method that is fast enough for in-line calculations while achieving accuracy comparable to single configuration Dirac-Fock results. The calculations use detailed term accounting; for example, the bound-bound transitions are treated in full intermediate or pure LS coupling depending on the element. Degeneracy and

plasma collective effects are included in inverse Bremsstrahlung and Thomson scattering. Most line broadening is treated with a Voigt profile that accounts for Doppler, natural width, and electron impacts. Linear Stark broadening by the ions is included for one-, two-, and three-electron systems. By contrast to the average-atom approach, where ions are assumed to be fractionally occupied, in the OPAL code the plasma is treated as a mixture of atoms in discrete ionization states, thereby giving a more realistic description of individual lines and absorption edges. However the OPAL calculations can only be done for a limited range of ions.

Analysis of Al plasmas

Since the anomalous index of refraction results were first measured in Al plasmas [4,5] using X-ray laser interferometers we utilize the average atom code to analyze Al plasmas and compare against OPAL calculations. To simplify the analysis, the calculations are done for different temperatures but with a constant ion density of 10^{20} cm^{-3}. Since the fringe shifts are proportional to f_1 or $(1 - n)$ we compare the ratio of $(1 - n) / (1 - n_{free})$ where $n_{free} = 1 - (N_{elec} / 2N_{crit})$ is the index of refraction due only to the free electron contribution. If only the free electrons contribute to the index of refraction this ratio equals one and the traditional analysis is valid. Otherwise this ratio represents the ratio of the measured electron density to the actual electron density when one analyzes the interferometer experiment the traditional way assuming only free electrons contribute to the index of refraction.

Even though the calculations are done for a single ion density the ratio normalizes away the actual density and we expect the analysis to be valid over a wider range of densities. One limitation of the calculations is that both the average atom code and OPAL assume the electron, ion, and radiation temperatures are all equal and the plasma's ionization is in local thermodynamic equilibrium (LTE). If one calculates a dynamic plasma that is not in equilibrium, the ionization condition (Z*) is a better value to compare than the actual temperature of the plasma. Z* is the ionization condition of the plasma such that Z* = 1 means the average ion is singly ionized, 2 means double ionized, etc.

Figure 1(a) shows the ratio $(1 - n) / (1 - n_{free})$ versus photon energy for Al plasma with temperature of 2 eV. A dotted line is plotted at a ratio of 0 as a visual aid. The solid curve is from the average atom code while the dashed line is from the OPAL calculation. The Z* = 0.92 and 0.88 for the two codes, which means that the average ion is almost singly ionized. One immediately notices that the ratio is negative from 75 eV to 100 eV with typical values for the average atom code ranging from –1 to –4. This means the index of refraction of the plasmas is greater than one. At 84.46 eV, which is the energy of the Pd X-ray laser (14.68 nm), the ratio is –2.8 for the average atom code and –11 for OPAL. In the detailed analysis of Al done in Ref. 9 the ratio for singly ionized Al was –4.2. In all three calculations, a Mach-Zehnder or Fresnel bi-mirror interferometer as used in Refs. 4 and 5, would observe the fringes bend the opposite direction than was expected and by a larger distance than would be expected for the electron density being measured. Looking at lower energies, such as the 26.4 eV (46.9 nm) of the Ne-like Ar X-ray laser [6] that has been used for many interferometer experiments, the ratio is 2.6 for the average atom code and 3.5 for OPAL. An interferometer built at this wavelength would measure an electron density that was about 3 times larger than the actual density. It is striking that the ratio crosses one but differs significantly from one over most of the energy range. Even at low energies, such as 4.68 eV, which is the energy of the 4^{th} harmonic of the 1.06 μm Nd laser, the ratio is predicted to be –3.0 for the average atom code and –0.5 for OPAL. Now it is important to recognize that an average atom calculation will not have the position of the absorption lines and edges accurate enough to use the ratio to quantitatively analyze the experiments but it is an invaluable first step in understanding the validity of the experiments and approximating the potential corrections needed to understand the experiments. The OPAL calculations should have the energies closer to the actual values but each situation needs to be compared against measured line positions to determine more accurate values. Both codes also have uncertainties in the line widths of the many resonance lines that will affect the shape of the calculation of 1 – n.

In Fig. 1(b) we plot the ratio for a 10 eV Al plasma with Z* = 2.88 and 2.82, which is almost triply ionized Ne-like Al. In Ne-like Al the strong 3s – 2p resonance lines are centered at 77.07 eV [17]. The average atom calculation shows a strong feature at 73.0 eV due to these absorption lines while the OPAL results have the feature at 78.73 eV. One obtains a more accurate estimate of the ratio by shifting this feature a few eV for each calculation to agree with the experimentally observed values of the lines as was done for the detailed analysis in Ref. 9. In Fig. 1(b) the ratio at 84.46 eV is –2.4 and –0.8 for the average atom and OPAL codes, respectively, If one shifts the energy axis by 4.07 and –1.66 eV to match the position of the Ne-like resonance line, then the ratio becomes –0.9 and –0.4 for the average atom and OPAL codes, respectively. Ref. 9 predicted a ratio of –0.6 for triply ionized Al at this photon energy. All three analyses predict that the ratio is negative and that the index of refraction is greater than one. This is consistent with the fringe lines in an interferometer experiment bending the opposite direction than expected. It is important to note that the index of refraction of the Al plasma is predicted to be greater than one over a wide range of photon energies near 85 eV and plasma conditions from neutral to triply ionized.

Another important plasma property to consider is the absorption coefficient of the plasma since the optical photons or X-rays need to be able to penetrate the plasma if they are to be used for interferometer measurements. Figure 2 shows the absorption coefficient versus photon energy for Al plasma of temperature 10 eV with an ion density of 10^{20} cm^{-3} using the average atom code. For the region between 75 and 85 eV and also between 40 and 70 eV the absorption coefficient is less than 10 cm^{-1}. Since a typical interferometer experiment [4,5] uses 0.1 cm long plasma, this means the plasma will be optically thin to the X-rays. Keep in mind that the energy scale needs to be shifted about 5 eV to higher energy to agree with the experiments, so even the 89 eV Ag X-ray laser used in the experiments in Ref. 4 would have low absorption under these conditions.

As we continue to ionize the Al plasma Fig, 3(a) shows the ratio $(1 - n) / (1 - n_{free})$ versus photon energy for a 20 eV Al plasma with Z* = 4.64 and 4.46. Much of the complicated

structure is disappearing at energies near 84.6 eV but the ratio is still only 0.6 and 0.66 for the average atom and OPAL codes, respectively, and is in good agreement with the value of 0.5 that one interpolates from Ref. 9. In this case the fringes would bend the expected direction in an interferometer experiment but the measured value of the electron density would be low by 30 to 50%.

Finally, Fig. 3(b) shows the ratio for a 40 eV Al plasma with Z* = 7.64 and 7.55. The ratio is within 10% of unity for most of the figure with the exception of some weak resonances. One has to ionize almost 8 of the 13 electrons from Al in order to approach the free electron approximation for the index of refraction. This is the same conclusion reached in Ref. 9. The Al experiments highlight how the traditional equation for the index of refraction in a plasma is not valid over a large range of plasma conditions and photon energies. At optical photon energies near a few eV the free electron approximation to the index for Al plasmas does appear to be valid except for the single ionized case. The average atom code and OPAL code give very similar values for Z*. Both codes show similar trends for the ratio $(1 - n) / (1 - n_{free})$ and there is good quantitative agreement when the energy scale is shifted to agree with known experimental lines or edges.

Analysis of other plasmas using carbon, titanium, or palladium

Materials containing carbon, such as plastics, are commonly used in experiments so we looked at the index of refraction for carbon plasmas. Again we fix the ion density of the plasma at 10^{20} cm^{-3}. Figure 4(a) plots the ratio of $(1 - n) / (1 - n_{free})$ versus photon energy for C plasma with temperature of 2 eV. The figure is very complicated for photon energies below 30 eV. If we focus on the 84.46 eV energy of the Pd X-ray laser used in the interferometer experiments [5] at LLNL one observes that the ratio is 6.7 and 8.4 for the average atom and OPAL codes, respectively. This would result in an experiment that greatly overestimates the electron density of the plasma. For C plasma at 5 eV, as shown in Fig. 4(b), the ratio is 2.3 and 2.7 at 84.46 eV for the average atom and OPAL codes, respectively. Even at 10 eV, as shown in Fig. 5(a), where the

plasma is almost triply ionized, the ratio of $(1 - n) / (1 - n_{free})$ is 1.3 and 1.4 for the two codes from 60 to 100 eV so experiments done with these energies would overestimate the electron density by 30 to 40%. Figure 5(b) shows the ratio for C plasma at 20 eV, which is almost 4 times ionized. This plasma has a ratio of 1.02 and 1.03 at 84.46 eV for the average atom and OPAL codes, respectively. The C plasma needs to be ionized down to the K shell before the free electron contribution dominates the index of refraction in this energy range. If we look at higher photon energies near the K edges the ratio will again deviate substantially from 1.

Ti plasmas have been studied for many reasons including their use as X-ray lasers [24]. Figure 6 shows the ratio $(1 - n) / (1 - n_{free})$ versus photon energy for Ti plasmas with temperatures of 5 and 40 eV using the average atom code. Again we fix the ion density of the plasma at 10^{20} cm^{-3}. At 5 eV the plasma is about doubly ionized and the ratio is about 4 over the 80 to 100 eV photon range, meaning an interferometer experiment using this photon energy would overestimate the electron density by a factor of 4. One needs to be almost 10 times ionized, as shown for the 40 eV curve, to have the ratio approach one over most of the plot. Even then there is a resonance near 100 eV that significantly changes the results if you are close enough.

Ni-like Pd [25] has been used very successfully as an X-ray laser for many years and currently is used as the laser source for the interferometer measurements at LLNL. Recently we conducted experiments [26] to measure the plasma conditions [27] of the Ni-like Pd X-ray laser just prior to lasing. The Pd laser is created by using a prepulse to illuminate a solid target that heats and expands to create plasma at the correct density and ionization to lase. A short, high-intensity pulse then rapidly heats the plasma to lasing conditions and finishes ionizing regions of the plasma that are slightly under-ionized to create the 18 times ionized Ni-like Pd plasma. Figure 7 shows the ratio $(1 - n) / (1 - n_{free})$ versus photon energy for Pd plasmas at 20 and 80 eV with $Z^* = 7.2$ and 17.8 respectively. The ion density of the plasma is fixed at 10^{20} cm^{-3}. At a photon energy of 84.46 eV, Fig. 7 shows the ratio is 2.6 for the 20 eV plasma and is 1.0 for the

80 eV plasma. From this figure one can see how even 7 times ionized Pd has a large contribution to the index of refraction from the bound electrons. By the time the plasma is ionized to Ni-like Pd, the ratio approaches one over this entire energy range except for some small resonances. Since the Pd plasma may be a few times less ionized than Ni-like in the interferometer experiments [27] that measure the condition of the Pd plasma created by the prepulse, we calculated the ratio for a 60 eV Pd plasma with Z* = 15.4. At 84.46 eV the ratio is 1.05 so the interferometer experiments could slightly overestimate the electron density by about 5% if the plasma is only 15 times ionized. These calculations show how the average atom code can be used to verify that interferometer experiments are being done in a regime where the free electron approximation is valid. The calculations also enable us to estimate the magnitude of the contribution from the bound electrons.

Conclusions

For decades the analysis of plasma diagnostics such as interferometers have relied on the approximation that the index of refraction of a plasma is due solely to the free electrons. This makes the index of refraction less than one and is also an essential assumption used in energy deposition in the plasma and for photon transport calculations. Recent X-ray laser interferometer measurements of Al plasmas observed anomalous results with the index of refraction being greater than one. The analysis of the Al plasmas show that the anomalous dispersion from both the resonance lines and absorption edges due to the bound electrons can have the dominant contribution to the index of refraction over the photon range from the optical up to 100 eV (12 nm) soft X-rays. It is well known that a strong resonance line can cause anomalous results near the absorption line but this work shows that the effects from the resonance lines extend to photon energies located orders of magnitude further from the line centers than the corresponding line widths owing to the fact that they contribute through a dispersion integral. Similar long-range effects are shown for the absorption edges.

Utilizing a new average atom code we calculate the index of refraction in C, Al, Ti and Pd plasmas and show many conditions over which the bound electron contribution dominates the free electrons as we explore photon energies from the optical to 100 eV soft X-rays. The average-atom calculations are validated against the more detailed OPAL results for carbon and aluminum plasmas. During the next decade X-ray free electron lasers and other sources will be available to probe a wider variety of plasmas at higher densities and shorter wavelengths so it will be even more essential to understand the index of refraction in plasmas. X-ray laser interferometers may become a valuable tool to measure the index of refraction of plasmas in the future.

Acknowledgements

The authors would like to thank K. T. Cheng who made valuable suggestions in the process of preparing this work. This work was performed under the auspices of the U. S. Department of Energy by the University of California Lawrence Livermore National Laboratory under contract No.W-7405-ENG-48. This research was also sponsored by the National Nuclear Security Administration under the Stewardship Science Academic Alliances program through U. S. Department of Energy Research Grant # DE-FG03-02NA00062. The work of one author (WRJ) was supported in part by NSF Grant No. PHY-0139928.

References

[1] G. J. Tallents, J. Phys. D. **17**, 721 (1984).

[2] H. R. Griem, *Principles of Plasma Spectroscopy*, (Cambridge University Press, Cambridge, 1997) p. 9

[3] L. B. Da Silva, T. W. Barbee, Jr., R. Cauble, P. Celliers, D. Ciarlo, S. Libby, R. A. London, D. Matthews, S. Mrowka, J. C. Moreno, D. Ress, J. E. Trebes, A. S. Wan, and F. Weber, Phys. Rev. Lett. **74**, 3991 (1995).

[4] H. Tang, O. Guilbaud, G. Jamelot, D. Ros, A. Klisnick, D. Joyeux, D. Phalippou, M. Kado, M. Nishikino, M. Kishimoto, K. Sukegawa, M. Ishino, K. Nagashima, and H. Daido, Appl. Phys. B **78**, 975 (2004).

[5] J. Filevich, J. J. Rocca, M. C. Marconi, S. Moon, J. Nilsen, J. H. Scofield, J. Dunn, R. F. Smith, R. Keenan, J. R. Hunter, and V. N. Shlyaptsev, "Observation of a multiply ionized plasma with index of refraction greater than one," University of California report UCRL-JRNL-207242, submitted to Phys. Rev. Lett. (2004).

[6] J. Filevich, K. Kanizay, M. C. Marconi, J. L. A. Chilla, and J. J. Rocca, Opt. Lett **25**, 356 (2000).

[7] D. Descamps, C. Lyngå, J. Norin, A. L'Hullier, C.-G. Wahlström, J.-F. Hergott, H. Merdji, P. Salières, M. Bellini, and T. W. Hänsch, Opt. Lett. **25**, 135 (2000).

[8] A. Meseck, M. Abo-Bakr, D. Krämer, B. Kuske, and S. Reiche, Nucl. Inst. And Meth. A **528**, 577 (2004).

[9] J. Nilsen and J. H. Scofield, Opt. Lett. **29**, 2677 (2004).

[10] D. A. Liberman, JQSRT **27**, 335 (1982).

[11] W. R. Johnson, C. Guet, and G. F. Bertsch "Optical properties of plasmas based on an average-atom model," see article in this issue of J. Quant. Spectrosc. Radiat. Transfer (2005).

[12] C. A. Iglesias, F. J. Rogers, and B. G. Wilson, Astrophys. J. Lett. **322**, L45 (1987).

[13] F. J. Rogers, B. G. Wilson, and C. A. Iglesias, Phys. Rev. A **38**, 5007 (1988).

[14] C. A. Iglesias and F. J. Rogers Astrophys. J. **464**, 943 (1996).

[15] A. Aguilar, J. B. West, R. A. Phaneuf, R. L. Brooks, F. Folkmann, H. Kjeldsen, J. D. Bozek, A. S. Schlachter, and C. Cisneros, Phys Rev A **67**, 012701 (2003).

[16] J. B. West, J. Phys. B **34**, R45 – R91 (2001).

[17] I. M. Savukov, J Phys B **36**, 4789 - 4797, (2003).

[18] B. L. Henke, E. M. Gullikson, and J. C. Davis, ADNDT **54**, 181 - 342 (1993).

[19] L. D. Landau and E. M. Lifshitz, *Electrodynamics of Continuous Media*, (Pergamon, New York, 1984) pp. 280 - 283

[20] D. A. Greenwood, Proc. Phys. Soc. London **715**, 585 (1958).

[21] R. Kubo, J. Phys. Soc. Jpn. **12**, 570 (1957).

[22] M. P. Desjarlais and J. D. Kress and L. A. Collins, Phys. Rev. E **66**, 025401(R) (2002).

[23] V. Recoules and P. Renaudin and J. Clèouin and P. Noiret and G. Zèrah, Phys. Rev. E **66**, 056412 (2002).

[24] Joseph Nilsen, Brian J. MacGowan, Luiz B. Da Silva, and Juan C. Moreno, Phys. Rev. A **48**, 4682 (1993).

[25] J. Dunn, Y. Li, A. L. Osterheld, J. Nilsen, J. R. Hunter, and V. N. Shlyaptsev, Phys. Rev. Lett. **84**, 4834 (2000).

[26] R.F. Smith, J. Dunn, J. Filevich, S. Moon, J. Nilsen, R. Keenan, V.N. Shlyaptsev, J.J. Rocca, J.R. Hunter, R. Shepherd, R. Booth, and M.C. Marconi, "Improved energy coupling into the gain region of the Ni-like Pd transient collisional x-ray laser," submitted to Phys. Rev. Lett. (2004).

[27] J. Nilsen, J. Dunn, R. F. Smith, T. W. Barbee, Jr., J. Opt. Soc. Am. B **20**, 191 (2003).

Figure Captions

Fig. 1. Ratio (1-n) / (1-n_{free}) versus photon energy for Al plasmas with temperatures of (a) 2 eV and (b) 10 eV. The solid curve is from the average atom code and the dashed line is from the OPAL code. The average ionization state is given by Z*. The ion density is 10^{20} cm^{-3}. The dotted line at a ratio of 0 is a visual aid.

Fig. 2. Absorption coefficient versus photon energy for Al plasma with temperature of 10 eV. The ion density is 10^{20} cm^{-3}.

Fig. 3. Ratio (1-n) / (1-n_{free}) versus photon energy for Al plasmas with temperatures of (a) 20 eV and (b) 40 eV. The solid curve is from the average atom code and the dashed line is from the OPAL code. The average ionization state is given by Z*. The ion density is 10^{20} cm^{-3}.

Fig. 4. Ratio (1-n) / (1-n_{free}) versus photon energy for C plasmas with temperatures of (a) 2 eV and (b) 5 eV. The solid curve is from the average atom code and the dashed line is from the OPAL code. The average ionization state is given by Z*. The ion density is 10^{20} cm^{-3}.

Fig. 5. Ratio (1-n) / (1-n_{free}) versus photon energy for C plasmas with temperatures of (a) 10 eV and (b) 20 eV. The solid curve is from the average atom code and the dashed line is from the OPAL code. The average ionization state is given by Z*. The ion density is 10^{20} cm^{-3}.

Fig. 6. Ratio (1-n) / (1-n_{free}) versus photon energy for 5 and 40 eV Ti plasmas with Z* = 2.2 and 9.9, respectively. The calculations are from the average atom code. The ion density is 10^{20} cm^{-3} for the Ti plasmas.

Fig. 7. Ratio (1-n) / (1-n_{free}) versus photon energy for 20 and 80 eV Pd plasmas with Z* = 7.2 and 17.8, respectively. The calculations are from the average atom code. The ion density is 10^{20} cm^{-3} for the Pd plasmas.

Table 1. The optical constant f_1 for different isoelectronic stages of Al at a photon energy 84.46 eV (14.7 nm). The total value of f_1 for a particular ionization stage is the sum of the contributions from the lines and continuum of the bound electrons together with the number of free electrons (Z*).

Ion	L3 edge (eV)	Line	Continuum	Free	f_1(total)
+0	73.1	+2.61	-3.46	+0	-0.85
+1	92.4	-0.70	-4.48	+1	-4.19
+2	105.4	-2.91	-2.63	+2	-3.54
+3	120.0	-3.16	-1.64	+3	-1.80
+4	153.7	-2.49	-0.66	+4	+0.84
+5	190.5	-1.17	-0.29	+5	+3.54
+6	241.4	-0.57	-0.13	+6	+5.30
+7	284.6	-0.20	-0.06	+7	+6.73
+8	330.2	+0.03	-0.03	+8	+8.00
+9	398.6	+0.19	-0.02	+9	+9.18

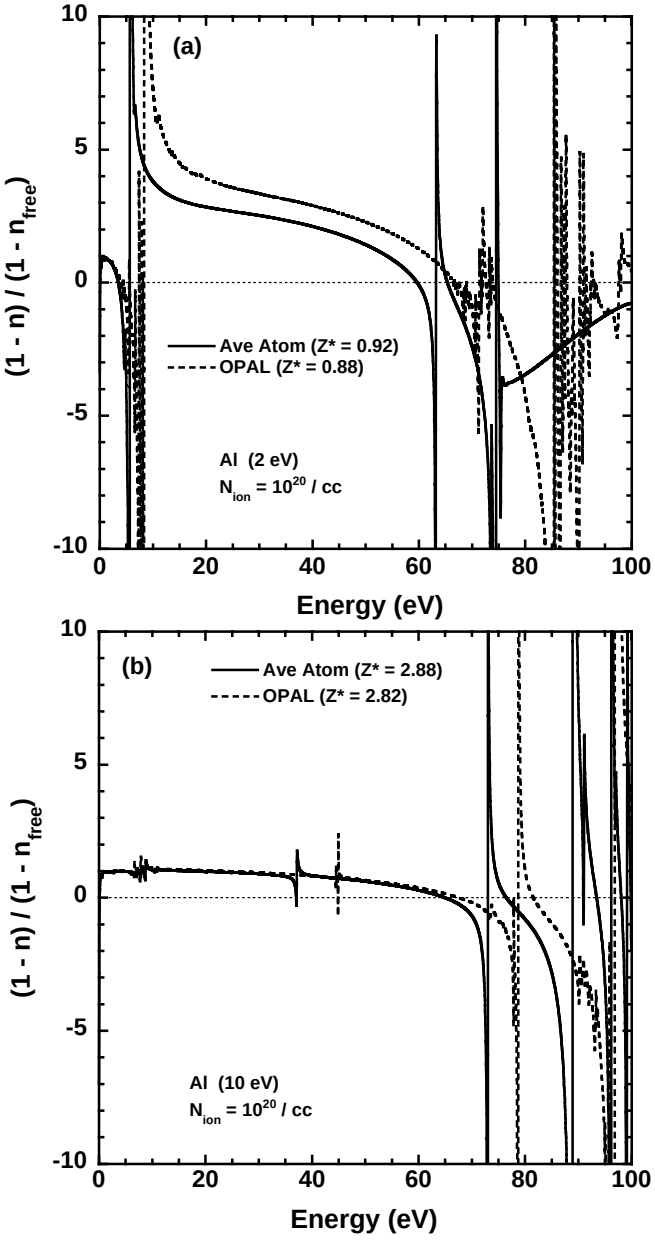

Fig. 1. Ratio (1-n) / (1-n_{free}) versus photon energy for Al plasmas with temperatures of (a) 2 eV and (b) 10 eV. The solid curve is from the average atom code and the dashed line is from the OPAL code. The average ionization state is given by Z*. The ion density is 10^{20} cm^{-3}. The dotted line at a ratio of 0 is a visual aid.

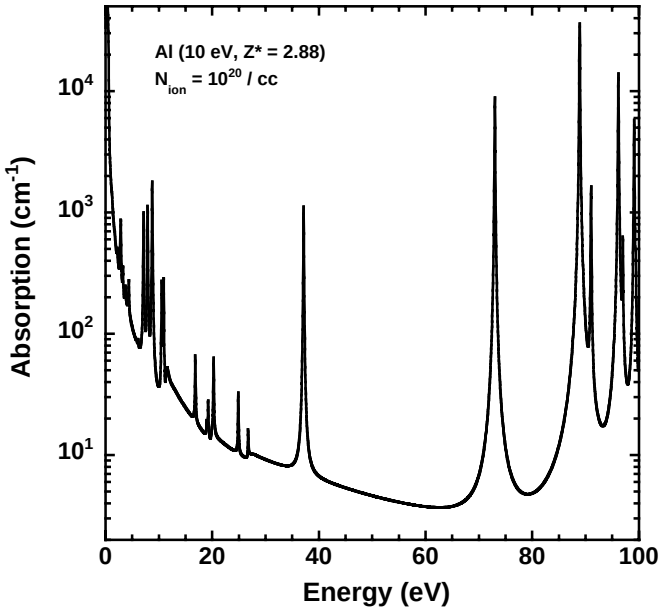

Fig. 2. Absorption coefficient versus photon energy for Al plasma with temperature of 10 eV. The ion density is 10^{20} cm^{-3}.

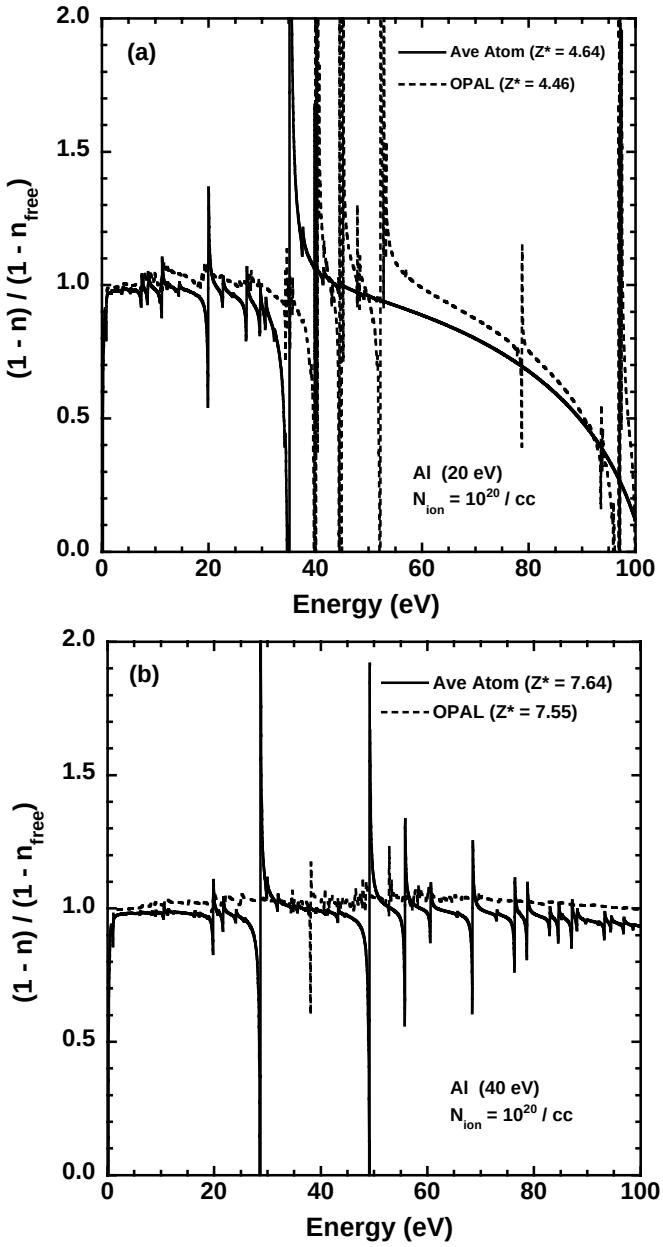

Fig. 3. Ratio (1-n) / (1-n_{free}) versus photon energy for Al plasmas with temperatures of (a) 20 eV and (b) 40 eV. The solid curve is from the average atom code and the dashed line is from the OPAL code. The average ionization state is given by Z*. The ion density is 10^{20} cm^{-3}.

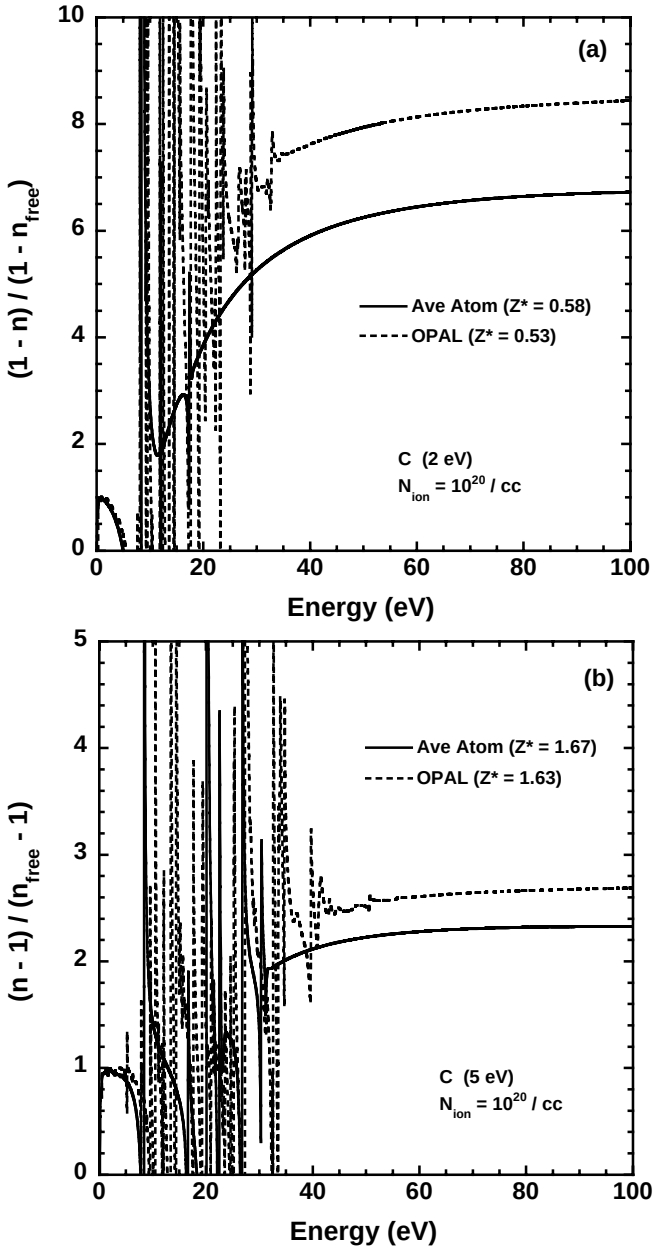

Fig. 4. Ratio (1-n) / (1-n_{free}) versus photon energy for C plasmas with temperatures of (a) 2 eV and (b) 5 eV. The solid curve is from the average atom code and the dashed line is from the OPAL code. The average ionization state is given by Z*. The ion density is 10^{20} cm^{-3}.

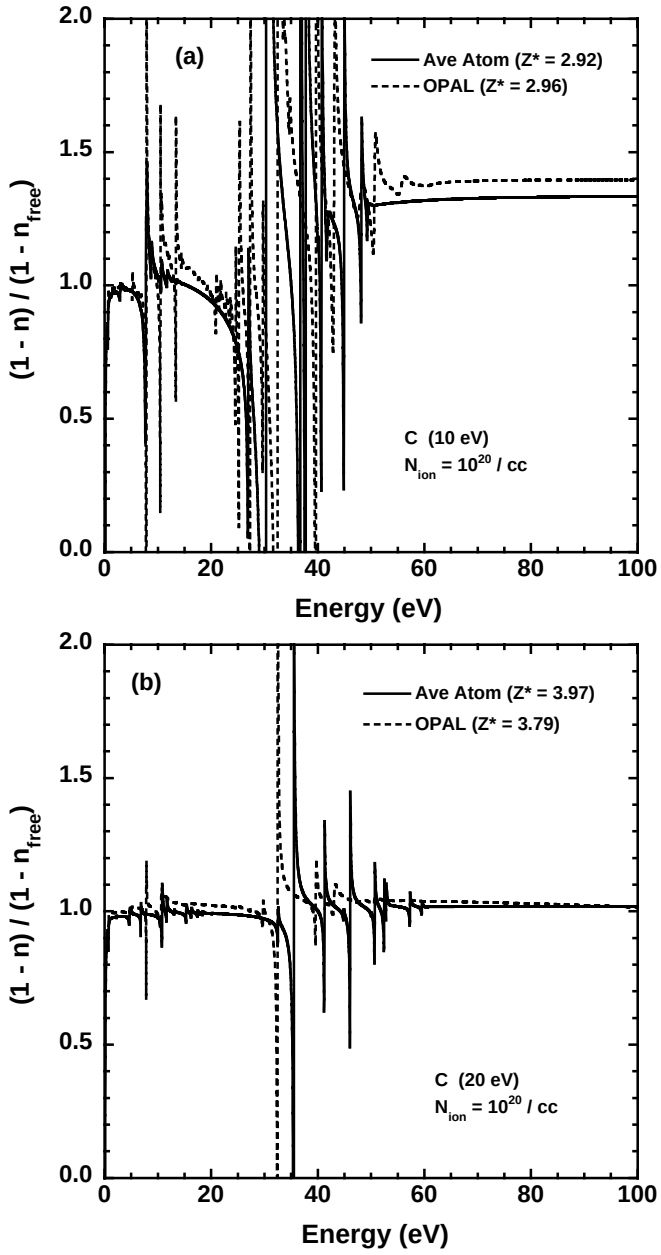

Fig. 5. Ratio (1-n) / (1-n_{free}) versus photon energy for C plasmas with temperatures of (a) 10 eV and (b) 20 eV. The solid curve is from the average atom code and the dashed line is from the OPAL code. The average ionization state is given by Z*. The ion density is 10^{20} cm^{-3}.

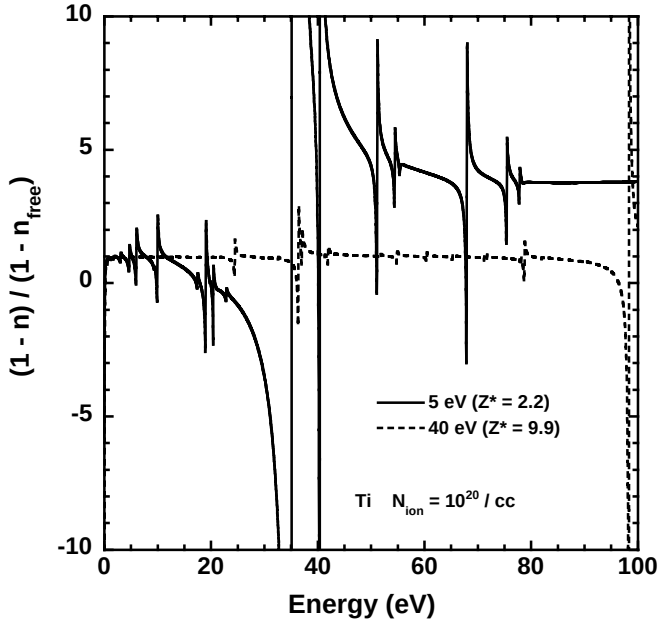

Fig. 6. Ratio (1-n) / (1-n_{free}) versus photon energy for 5 and 40 eV Ti plasmas with Z* = 2.2 and 9.9, respectively. The calculations are from the average atom code. The ion density is 10^{20} cm^{-3} for the Ti plasmas.

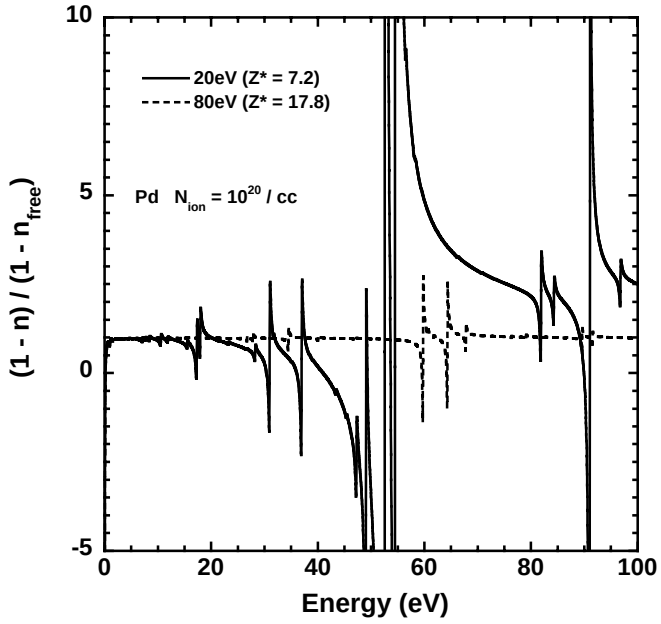

Fig. 7. Ratio (1-n) / (1-n_{free}) versus photon energy for 20 and 80 eV Pd plasmas with Z* = 7.2 and 17.8, respectively. The calculations are from the average atom code. The ion density is 10^{20} cm^{-3} for the Pd plasmas.